



# Effect of cage size on oxygen levels in Atlantic salmon sea cages: A model study

Morten Omholt Alver<sup>\*</sup>, Martin Føre, Jo Arve Alfredsen

NTNU Department of Engineering Cybernetics, 7491 Trondheim, Norway

## ARTICLE INFO

### Keywords:

Mathematical model  
Hypoxia  
Exposed aquaculture  
Advection-diffusion equation  
Scale  
Current speed

## ABSTRACT

The supply of dissolved oxygen (DO) to salmon in sea cages depends on many interacting factors including biomass density, temperature and current speed. With other factors being equal, hypoxic conditions are more likely to arise in large cages compared to small. In this work, a mathematical model of DO in sea cages is used to analyse the effect of horizontal cage size in particular. It is shown and quantified how the DO level at key locations in the cage depend on cage radius and current speed, and the fraction of the cage volume with hypoxic conditions is estimated as a function of cage radius, current speed and temperature.

The results of this study give new insight into how oxygen conditions are affected when cage size is scaled up or down. Although conditions at actual aquaculture sites are highly variable and complex, the results can help forecast the effect of increasing cage size at existing sites, and can help guide the planning of new production sites with regard to oxygen supply.

## 1. Introduction

The salmon aquaculture industry is one of the most successful sectors within intensive aquaculture, with more than 2.7 mill tonnes produced globally in 2020 (FAO, 2022). Based on the dual goal of increasing productivity and expanding production into more exposed and remote areas (Bjelland et al., 2015), the industry has recently pushed towards ever increasing cage sizes as recently discussed by McIntosh et al. (2022). Larger cages are likely to result in higher efficiency and per capita production, as the crew required to manage a cage and other input factors will not necessarily scale linearly with the size of the cage. However, the cage environment is also dependent on cage size, and factors that vary in the three dimensional space, such as dissolved oxygen (DO), are particularly sensitive to scale changes. When cage size increases, the surface area to volume ratio of the cage declines, and the relative water exchange rate is reduced (Klebert et al., 2013). This effect may be further strengthened by cage operations actively inhibiting water exchange, such as lice skirts. Jónsdóttir et al. (2021) measured currents and DO levels in a cage with 25 m radius with and without a lice skirt, and found that using skirts reduced current speeds and DO levels inside the cage compared to outside. For cages without lice skirts, Oldham et al. (2018) compared measurements of DO levels in cages of approximately 27 and 38 m radius, concluding that average DO levels

were slightly lower in the larger cages, but also that conditions were acceptable in the larger cages as long as the environmental conditions were sufficiently favourable. Although this provides some qualitative observations on how DO conditions may vary with cage scale, there have been few studies targeting how increased cage size impacts the production environment.

To the authors' knowledge, low oxygen levels has not been documented as a significant problem today in open cage systems in Norway. In Tasmania's Macquarie Harbour, the summer months have been identified as a critical production period due to the combination of high temperatures and low oxygen levels (Dempster et al., 2016). This is for instance seen in the data of Stehfest et al. (2017) from cages of approximately 25 m radius. Oxygen is also a significant challenge in Chile, partly related to the lack of strict biomass management and carrying capacity considerations, as discussed in the review by Quiñones et al. (2019). Burt et al. (2012) documented relatively frequent hypoxic events at one of their test sites in Newfoundland in Canada.

While sub-optimal oxygen conditions are known to adversely affect the physiology and ultimately health of fish (Remen et al., 2013, 2016), the ability of salmon to actively avoid detrimental DO levels has not been as clearly established as their ability to avoid other adverse conditions (Oppedal et al., 2011). Experimental findings on this area are somewhat contrasting. For instance, Johansson et al. (2006, 2007)

<sup>\*</sup> Corresponding author.

E-mail address: [morten.alver@ntnu.no](mailto:morten.alver@ntnu.no) (M.O. Alver).

<https://doi.org/10.1016/j.aquaculture.2022.738831>

Received 30 April 2022; Received in revised form 7 September 2022; Accepted 11 September 2022

Available online 16 September 2022

0044-8486/© 2022 The Author(s). Published by Elsevier B.V. This is an open access article under the CC BY license (<http://creativecommons.org/licenses/by/4.0/>).

investigated a range of environmental factors, including temperature, current and dissolved oxygen, outside and within sea cages, and observed the fish distributions in relation to those factors. No avoidance of low DO conditions was found in these studies, but it should be noted that oxygen saturation did not go notably beneath 80% in either of the experiments. In contrast, Oldham et al. (2017) found that salmon have some capacity to modify their behaviour in response to intermediate DO levels, but that this response may be overridden by the response to other environmental cues, such as temperature. Stehfest et al. (2017) used telemetry tags to track salmon movements due to temperature and DO variations, providing an individual based angle on this topic. Their findings indicated that salmon tend to avoid areas with low oxygen saturation, particularly below 35%. Based on these observations, it is reasonable to assume that farmed Atlantic salmon can sense adverse DO levels, and that they are likely to move away from severely hypoxic regions. On the other hand, the fish do not seem to efficiently avoid moderately hypoxic conditions, underlining the importance of ensuring sufficient DO levels in the entire cage volume.

It is challenging to isolate the effect of increasing cage size in field experiments, since there can be numerous confounding factors such as current speed and other oceanographic conditions, differences in local farm conditions and changes in fish behaviour caused by outside effects. While this renders experimental investigation difficult, it is a good case for a mathematical modelling and simulation study where all variables can be controlled through model setup and initialisation. Such virtual studies have for instance been conducted to assess scaling effects in fish growth in tanks (Føre et al., 2018a), using a combined fish behaviour (Føre et al., 2009) and feed distribution Alver et al. (2016) model. Alver et al. (2022) developed a mathematical model of DO levels in sea cages based on the advection-diffusion equation combined with a feed distribution model and assumptions on the distribution of fish, which was set up for a large-scale offshore farm and validated using measurements. Since the model includes the basic mechanics of oxygen transport and consumption, it is well suited for isolating and investigating the effect of cage scale on DO levels.

The main aim of this study was to explore how the horizontal radius of a fish cage affects the internal values of dissolved oxygen within the cage. This was done by applying the model from Alver et al. (2022) to a set of different horizontal cage sizes while keeping the cage depth, fish biomass density, current speed and feeding rate per unit biomass constant across all simulations. As current speed is an important determinant of dissolved oxygen levels within a cage, the scaling effects were also tested over a range of current speeds. Fish behaviour in the form of the fish avoiding areas with low oxygen levels was taken into account to increase the realism of the simulations.

## 2. Materials and methods

This study uses a modified version of the model presented by Alver et al. (2022). The model was originally derived to simulate pellet distributions in sea cages (Alver et al., 2004, 2016), but has also been adapted to predict variations in DO by validation using data from a large-scale offshore sea cage (Alver et al., 2022).

### 2.1. Model description

The model is described in detail in Alver et al. (2022), but a brief summary is given here. The 3D field of dissolved oxygen, represented by  $\omega(x, y, z, t)$ , where  $x$ ,  $y$  and  $z$  are spatial dimensions and  $t$  is time, is modelled using the advection-diffusion equation:

$$\frac{\partial \omega}{\partial t} + v_x \frac{\partial \omega}{\partial x} + v_y \frac{\partial \omega}{\partial y} + v_z \frac{\partial \omega}{\partial z} + \kappa_h \left( \frac{\partial^2 \omega}{\partial x^2} + \frac{\partial^2 \omega}{\partial y^2} \right) + \kappa_v \left( \frac{\partial^2 \omega}{\partial z^2} \right) = \alpha - \sigma \quad (1)$$

where  $v_x$ ,  $v_y$  and  $v_z$  are current speed components,  $\kappa_h$  and  $\kappa_v$  are diffusion coefficients,  $\alpha$  the addition rate of oxygen (only relevant if oxygen

diffusors are used) and  $\sigma$  the spatial distribution of the oxygen consumption rate.

The oxygen consumption rate per fish is modelled as:

$$V_{O_2} = 1.3 \cdot 0.0171 W^{-0.33} 1.03^T 1.79^U \quad (2)$$

where  $W$  is body weight (kg),  $T$  is water temperature ( $^{\circ}\text{C}$ ) and  $U$  is swimming speed (1 body length per second is assumed in this study), partly based on the model of Grøttum and Sigholt (1998). The fish is represented through a set of 7 groups forming a population approximating a normal distribution for body weight, and the total oxygen consumption is computed as the sum of the contributions of each group.

The spatial distribution of oxygen consumption is based on a uniform distribution for non-feeding fish. When feeding, the distribution of feed is modelled as in Alver et al. (2016). Feed ingestion rate depends on spatial feed distribution and on the appetite of each of the fish groups, which in turn depends on gut fullness, so the ingestion rate will drop off as the fish becomes satiated. A 25% fraction of the population is assumed to be actively feeding at any time, and assumed to distribute proportionally with the feed. The contributions from the feeding and non-feeding fractions of the population form the total distribution of oxygen consumption represented by the  $\sigma$  term.

### 2.2. Model configuration

#### 2.2.1. Physical environment

The simulated fish cage is cylinder shaped with a flat bottom, and spans a depth of 30 m. Each simulation features a single cage, defined within a model domain set up as a rectangular prism with horizontal and vertical dimensions slightly larger than those of the cage itself to ensure that the domain properly covers the entire cage. The model domain is discretised into a 3D grid of cells in accordance with the horizontal and vertical resolutions which are both set at 2 m. Any cell whose center is within the cage radius measured from the center of the model domain, is considered inside the cage; other cells are considered outside.

The current field in the model domain is assumed to be uniform with the same direction as the ambient current field. Speed in the cells considered inside the cage is reduced by 20% compared with the values outside the cage. This simulates the so-called wake effect where the water flow speed is dampened by passing through net panels (Kristiansen and Faltinsen, 2012; Endresen and Klebert, 2020). The resulting current vector is applied within the whole domain, even though some model cells are defined as outside of the cage. Since the wake effect is only caused by the water flowing through the net material, it is independent of the actual cage size. To isolate the scaling effect, the speed reduction and hence relationship between outside/inside currents is therefore kept constant across scales.

#### 2.2.2. Fish population and feeding

The fish population in all simulations is set up with an average weight of 5 kg ( $\pm 1$  kg), and a population size (i.e., number of individual fish) scaled to give a biomass density of 20 kg  $\text{m}^{-3}$  within the cage volume regardless of cage scale. When feeding is activated, the feed input is assumed to be uniformly distributed at the surface over a circle with half the cage's radius, meaning that the feeding covers 25% of the surface at all cage scales.

#### 2.2.3. Model modifications

The original version of the model assumes that the fish do not change their behaviour in response to DO levels. During feeding, the fraction of fish that is feeding at any time is assumed to follow the distribution of feed, while the non-feeding part of the population (or all the fish when feeding is not active) is assumed to be uniformly distributed throughout the cage. However, since there will be significant volumes with low DO concentration in parts of this model study, the model has been modified based on the results from Stehfest et al. (2017) such that the fish will

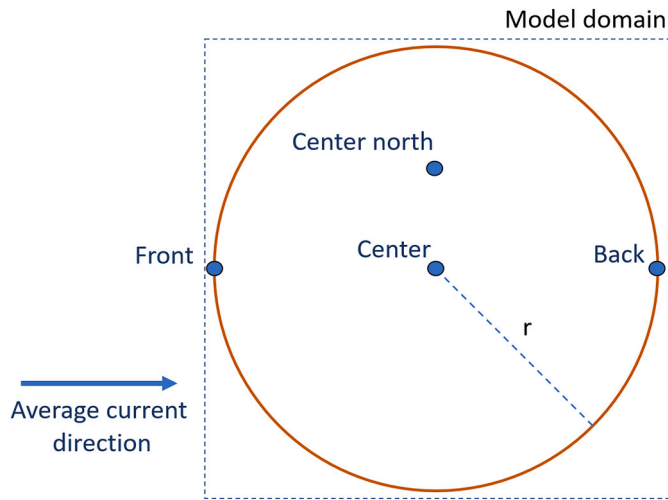


Fig. 1. Overview of cage and virtual sensor positions. Virtual sensors are placed at 4 m and 20 m depth at each of the four positions.

seek away from areas with low DO levels. This is implemented in the model through the *affinity* feature, where each model cell is assigned an affinity value  $a_{i,j,k}$  from 0 to 1 (where  $i, j$  and  $k$  are the coordinates of the cell). An affinity value specifies the propensity of the fish to stay in or avoid a particular location of the cage, with 0 meaning complete avoidance and 1 meaning no avoidance. The affinity value is multiplied with the feed ingestion or oxygen consumption value that would otherwise be used for each cell, to modulate these relative to the local

DO level. The rates in all cells are then scaled to ensure that the correct total feed ingestion and oxygen consumption rates for the population are still intact.

The affinity values are set as follows:

$$a_{i,j,k} = \begin{cases} 0, & \text{if outside of cage,} \\ 1, & \text{if inside and } \omega_{i,j,k} \geq \omega_{threshold} \\ \frac{\omega_{i,j,k}}{\omega_{threshold}}, & \text{if inside and } \omega_{i,j,k} < \omega_{threshold} \end{cases} \quad (3)$$

where  $\omega_{i,j,k}$  is the DO concentration in cell  $i, j, k$  and  $\omega_{threshold}$  the threshold value for DO beneath which the fish will respond with avoidance behaviour. These values serve to restrict fish presence to the volume inside of the cage, and to reduce their presence when the DO level goes below the threshold value.  $\omega_{threshold}$  is chosen as  $6 \text{ mg l}^{-1}$ , as that is often considered the limit for hypoxia for salmon (Burt et al., 2012). The affinity decrease is linear below  $\omega_{threshold}$ , but the actual reduction of fish presence will be smaller, especially if a significant portion of the cage volume is below  $\omega_{threshold}$ .

### 2.3. Simulation experiments

To test scaling effects, the model was set up to do simulation across seven different horizontal scales (10–70 m radius), each case featuring a range of current speeds and feeding vs. no feeding. Since temperature has an impact on both oxygen consumption in the fish and the saturation levels of oxygen in water, simulations were conducted for 12, 14 (nominal) and 16 °C. The resulting simulation setups can be summarised as follows:

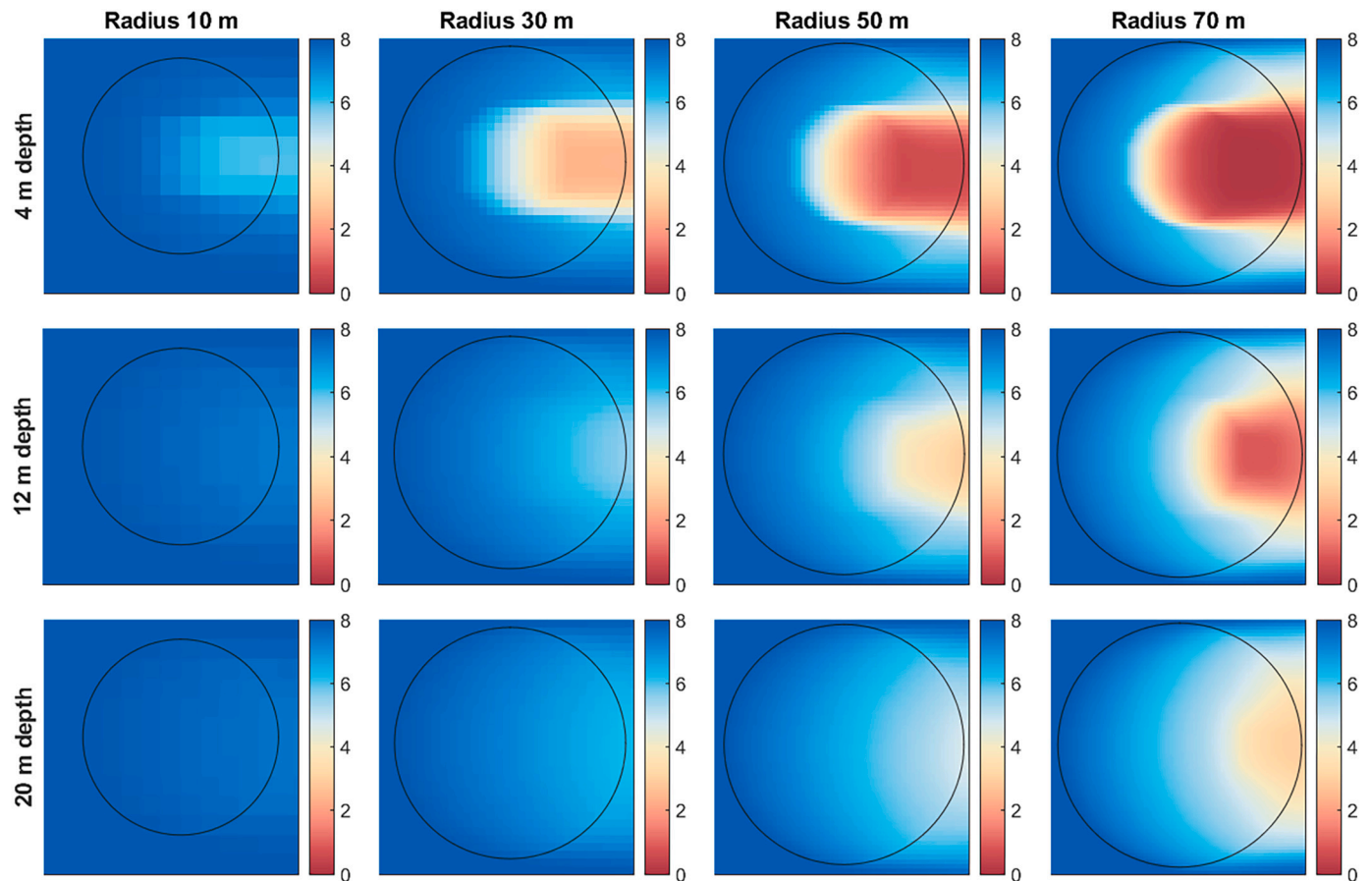


Fig. 2. Horizontal distribution of DO levels at a current speed of 0.03 m/s (towards the right in the figure) at three different depths and a selection of cage scales during feeding. Black circles indicate cage circumferences. Note that the horizontal scales of the plots differ between cage sizes.

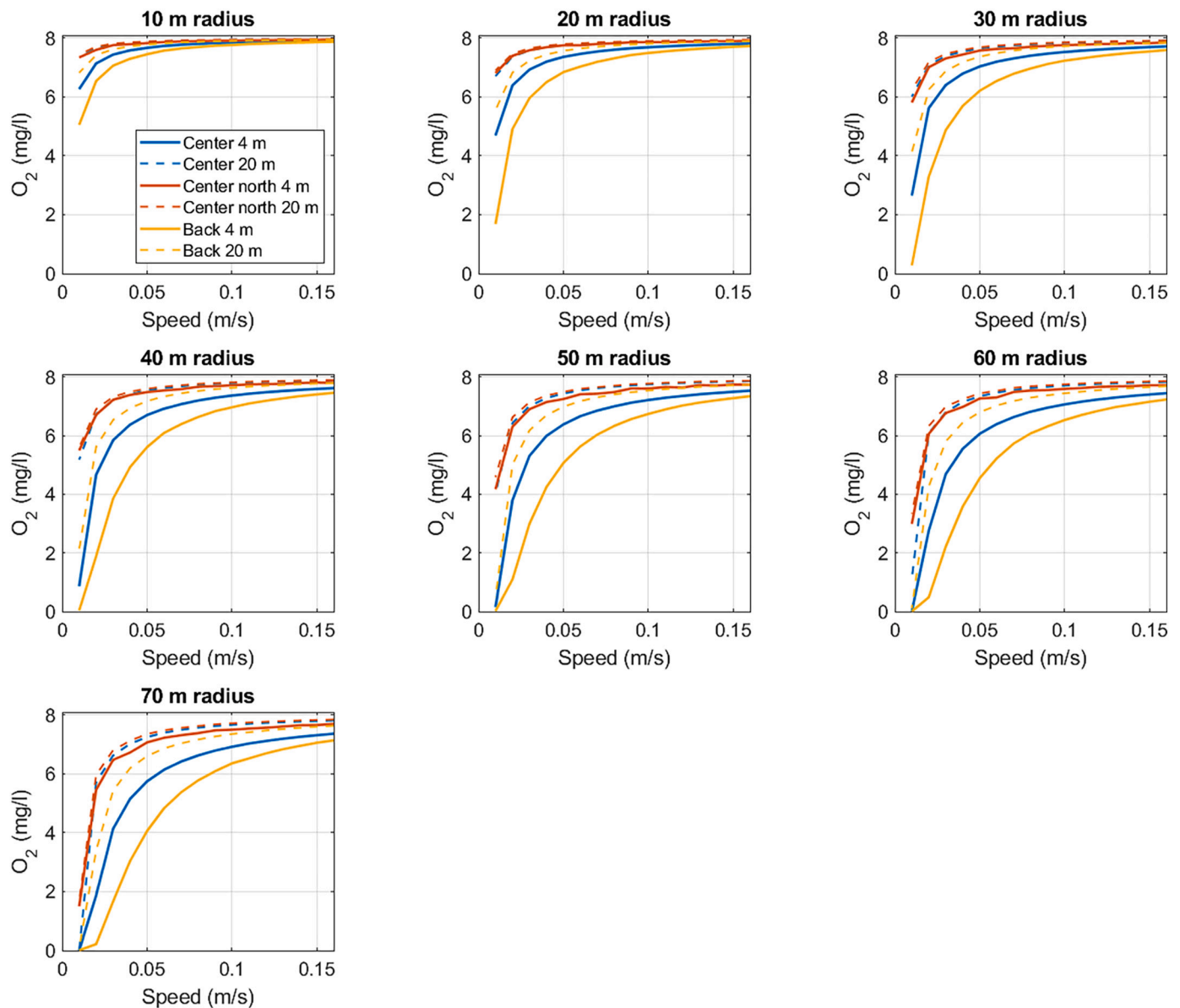


Fig. 3. Mean values at 4 m and 20 m sensor positions during feeding as a function of current speed and cage radius.

- Simulated cage radii: 10, 20, 30, 40, 50, 60 and 70 m.
- Simulation time 96 h (model time), with current speed starting at 0.16 m/s, and adjusted downwards by 0.01 m/s every 6 h.
- Each 6 h interval was split into non-feeding (first three hours) and feeding (last three hours) periods. At the start of each feeding period, the fish were reset to 0 gut content to ensure maximum appetite.
- Average current direction was set to be straight eastwards (90 degrees) with random variations modelled as a Gauss-Markov process with standard deviation of  $\sigma = 10$  degrees and autocorrelation function  $R_x(\tau) = \sigma^2 e^{-0.01|\tau|}$  (meaning the autocorrelation drops to approximately 37% of its maximum value at a time lag of 100 s).
- Constant ambient DO levels and temperature at all depths: 8 mg l<sup>-1</sup> at 14 °C, 8.33 mg l<sup>-1</sup> at 12 °C, and 7.69 mg l<sup>-1</sup> at 16 °C. Relative saturation was equal at the three temperatures.
- Time series (every 1 min) of DO level at selected virtual sensor positions within the cage (Fig. 1).
- Time series (every 1 min) of the fraction of model cells within the cage with DO level below  $\omega_{thresh}$ .
- Time series (every 1 min) of the average and minimum DO levels within the cage volume.
- Full 3D fields of DO levels (every 10 min).

For analysis, each simulation was split into 32 periods of 3 h each, representing a combination of the variables current speed (0.01–0.16 m/s) and feeding activated/deactivated. From each of these periods, the first 1.5 h are disregarded to give the model time to respond to new inputs and stabilise its outputs, while the model outputs are averaged over the last 1.5 h and used as the result from the analyses.

#### 2.4. Data analysis

The following model outputs were stored for analysis from each simulation:

#### 3. Results

In all simulations, DO levels within the cages were generally characterised by a gradual current speed-dependent decrease from ambient level from the upstream to the downstream cage wall along the current

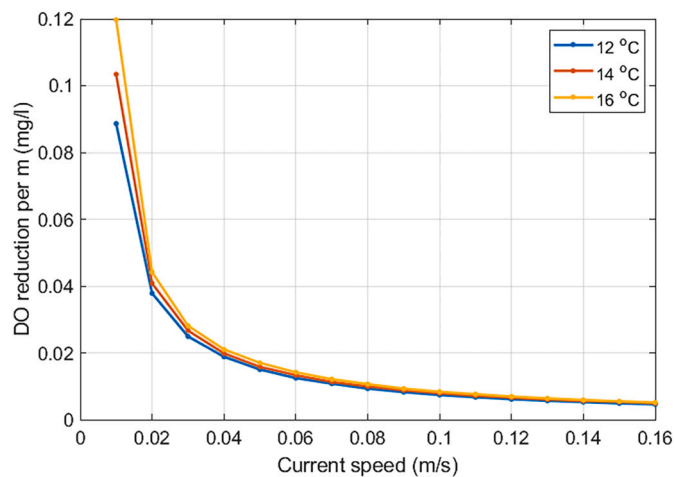


Fig. 4. Rate of decrease in DO level per m from the cage wall along the current direction near the surface under non-feeding conditions. Values for three different temperatures are shown.

direction. When feeding was activated, higher concentrations of fish within the feeding area led to a sharper decrease in that area, particularly in the upper 5–10 m of the water column where most of the feed is ingested. Fig. 2 shows examples for the case where feeding is activated and the current is quite slow (0.03 m/s).

Fig. 3 shows mean values seen at some of the sensor positions for all cage sizes and current speeds. For all cases, the virtual sensors placed at 4 m in the centre and downstream experience the largest reduction in DO. The sensors placed at 20 m were less affected and had generally higher DO levels. Note that for all scales, DO values were above  $\omega_{thresh} = 6 \text{ mg l}^{-1}$  for all sensors when the current speed was at least  $0.1 \text{ ms}^{-1}$ .

The horizontal rate of decrease of DO level seen along the current direction is independent of cage scale, and has been quantified for three different temperatures in non-feeding periods in Fig. 4. The values are calculated based on the reduction of DO in the uppermost layer of the model over a span from right inside the front of the cage to the center. Although this illustrates how temperature perturbs the decrease in oxygen due to fish consumption at low speeds, this difference clearly declines with higher speeds.

Fig. 5 summarises the predicted percentage of the cage volume with hypoxic conditions (DO level below  $\omega_{thresh} = 6 \text{ mg l}^{-1}$ ) under feeding conditions. Contour lines indicate what current speed is required to limit hypoxia for any cage radius, and the differences between the three

panels shows how temperature affects hypoxia.

## 4. Discussion

### 4.1. Relationship between cage scale and DO conditions

Upscaling of production units is one of the main trends in the intensive fish farming industry, but the full implications of this trend upon the production environment in sea cages is not fully understood. This study has shed some light on the relationship between physical scale and the likelihood of experiencing low oxygen conditions potentially detrimental for the fish through a series of simulation experiments. Although the experiments are purely virtual, the model used has been validated using real-world full-scale oxygen data from a cage (Alver et al., 2022) and is thus likely to capture the main dynamics of oxygen distribution in salmon cages.

Under the assumptions of the present model, a clear correspondence is seen between cage diameter and any of the measures of DO conditions that have been investigated. For any given cage diameter, a certain amount of current is required to ensure sufficient oxygen throughout most of the cage volume, and the values shown in Fig. 5 may serve as rough guidelines. Note that great care should be taken in using these predicted values except as indicators of how DO conditions scale with the cage diameter. For any given cage at a given location, many factors may strongly affect the actual DO conditions, especially the biomass density. The  $20 \text{ kg m}^{-3}$  used in this study represents a highly stocked cage at slaughter weight. Other factors are the ambient DO level, biofouling on the cage wall, lice skirts and the behaviour and feeding activity of the fish. However, if one has sufficient experience and knowledge of the DO levels typically encountered at a production site, the results of this study can be helpful in predicting the isolated effect of changing the cage size.

All results are presented as current dependent values due to the strong impact of current speed on DO levels inside the cage. If the current speed inside the cage is assumed to not be significantly affected by a change in cage diameter, one can compare different cage scales directly. It is worth noting that challenging DO conditions and strong effects of cage scale primarily occur at low current speeds. At a real location, current speeds tend to be highly variable in time, meaning that such low speeds will only occur over short intervals and not over periods up to 6 h as in the simulations. This means that the likelihood of encountering hypoxic DO levels in conventional farms will on average be low, and the effects of cage scale may hence not be so strong. However, potential problems occur at those times when current speed is low, and those are the times when cage scale has the strongest impact.

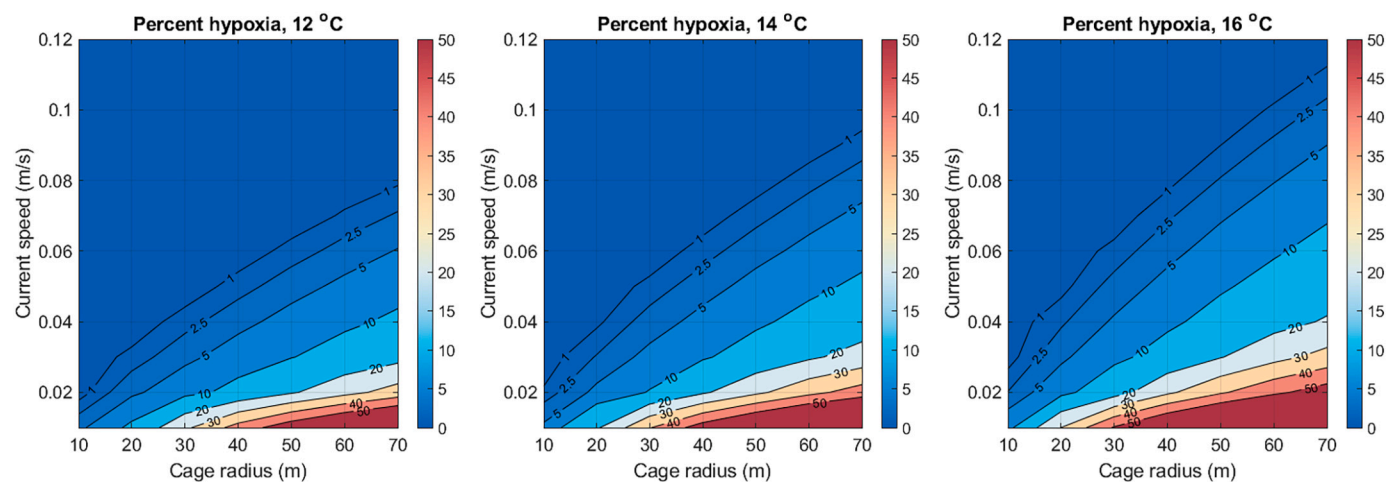


Fig. 5. Percentage of cage volume in hypoxic conditions (DO level below  $\omega_{thresh} = 6 \text{ mg l}^{-1}$ ) during feeding for three temperatures as a function of cage scale and current speed.

#### 4.2. Model limitations

The most important limitation of the model is its simplified representation of current conditions in the cage, and of the distribution of the fish biomass. The flow field inside a fish cage is clearly more complex than a uniform field, with turbulent motions both naturally present but also likely enhanced by the movements of the fish. Turbulent motion is implicit in the model through the diffusion term that represents turbulent mixing of the water, although the choice of correct diffusion coefficient is challenging. If there are systematic deviations in the inside flow field compared to the outside current vector, this will lead to model error. However, when using the model to isolate the effect of cage scale, such errors are likely to be of minor importance.

Two effects that modulate the oxygen consumption of the fish are not included in the model. The first is increased swimming speed during feeding. This effect is likely to be relatively small, judging from the results of Stockwell et al. (2021) who used acoustic telemetry to measure the swimming speed of Atlantic salmon, finding an increase ranging from 1.2% to 19.7% for feeding periods compared to non-feeding. The Grøttum and Sigholt (1998) model indicates a 12% increase in oxygen consumption at the upper end of this interval with 1 body length per second as base velocity. It is possible to include this effect in the model, but it is not likely to significantly affect the results of the scaling study. The second is elevated oxygen consumption associated with digestion activity. As feeding takes place during a part of each 24 h cycle, digestion activity, and consequently oxygen consumption rate, will vary throughout the day. The risk of seeing hypoxic conditions in a cage can be increased in the periods of highest digestive activity, thus making the worst case scenario worse than indicated by the results of the present study.

The model covers a single production unit only, while at real aquaculture sites there are usually several units placed relatively close together. If the wake from one unit passes through one or more other units, their DO conditions will suffer due to their input levels being reduced. These effects can be further explored by setting up a larger model domain covering a set of cages, thus explicitly modelling DO conditions for a complete farm.

#### 4.3. Model applications and future expansions

This work demonstrates the efficacy of using modelling studies to investigate phenomena that are difficult to explore through controlled field experiments, as in this case for the relationship between cage scale and DO conditions. Researchers must usually rely on commercially operated farms for field trials to get access to fully stocked large cages, and will then typically have limited control over the choice of basic farm infrastructure. One such comparison in the field was made by Oldham et al. (2018), who compared cages of 27 and 38 m radius and found a decrease in average DO of ca. 1% from the smaller to the larger cage (from  $90 \pm 0.02\%$  to  $89 \pm 0.03\%$  saturation). By comparison, this corresponds approximately to the decrease in average DO over the whole cage volume in the model from 30 to 40 m radius at a current speed of 0.06 m/s. However, the biomass density in the model study was much higher, the biomass density was lower in the 38 m cage than in the 27 m cage, and no information about the current speeds was given, so it is hard to assess the results. Given these challenges, a full experimental validation of scale effects is not likely to be available in the near future. But further validation of the present model for different scales, adding to the study of Alver et al. (2022), will be highly desirable in order to refine and increase confidence in the modelled scale effects.

Irrespective of scaling issues, the model may also be used as a tool for predicting the DO distribution in sea cages. Ultimately, such a model can help identify the various mechanisms behind oxygen distribution in sea cages, and thus increase human insight into the dynamics of fish farms, which is in line with the ideas of Precision Fish Farming (Føre et al., 2018b). Predictive models can also be used in what is known as virtual

prototyping, where the initial stages of the design and testing of a system is done through mathematical modelling and simulation instead of through physical prototypes (Wang, 2002). In this context, the present model could be used to virtually test how designing and scaling cages differently may impact the possibility of securing acceptable oxygen conditions for the fish.

Integrating the model with abilities to assimilate real time data from oxygen sensors using e.g. ensemble Kalman filters (Evensen, 2003) or nonlinear observer methods (Fossen, 1999) could further increase the realism and predictive power. This could also serve as a step towards realising a digital twin (Rasheed et al., 2020) of the processes in commercial fish farms, if combined with existing models of feed distribution (Alver et al., 2016), fish behaviour (Føre et al., 2009) and structural dynamics (Su et al., 2021).

#### Declaration of Competing Interest

The authors declare that they have no known competing financial interests or personal relationships that could have appeared to influence the work reported in this paper.

#### Data availability

Data will be made available on request.

#### Acknowledgements

Martin Føre acknowledges the financial support from Salmar ASA/Salmar Aker Ocean AS.

#### References

- Alver, M.O., Alfredsen, J.A., Sigholt, T., 2004. Dynamic modelling of pellet distribution in Atlantic salmon (*Salmo salar* L.) cages. *Aquac. Eng.* 31, 51–72. <https://doi.org/10.1016/j.aquaeng.2004.01.002>.
- Alver, M.O., Skoien, K.R., Føre, M., Aas, T.S., Oehme, M., Alfredsen, J.A., 2016. Modelling of surface and 3d pellet distribution in Atlantic salmon (*Salmo salar* L.) cages. *Aquac. Eng.* 72, 20–29. <https://doi.org/10.1016/j.aquaeng.2016.03.003>.
- Alver, M.O., Føre, M., Alfredsen, J.A., 2022. Predicting oxygen levels in Atlantic salmon (*Salmo salar*) sea cages. *Aquaculture* 548, 737720. <https://doi.org/10.1016/j.aquaculture.2021.737720>.
- Bjelland, H.V., Føre, M., Lader, P., Kristiansen, D., Holmen, I.M., Fredheim, A., Grøtli, E. I., Fathi, D.E., Oppedal, F., Utne, I.B., et al., 2015. Exposed aquaculture in Norway. In: *OCEANS 2015-MTS/IEEE Washington*. IEEE, pp. 1–10. <https://doi.org/10.23919/oceans.2015.7404486>.
- Burt, K., Hamoutene, D., Mabrouk, G., Lang, C., Puestow, T., Drover, D., Page, F., 2012. Environmental conditions and occurrence of hypoxia within production cages of Atlantic salmon on the south coast of Newfoundland. *Aquac. Res.* 43, 607–620. <https://doi.org/10.1111/j.1365-2109.2011.02867.x>.
- Dempster, T., Wright, D., Oppedal, F., 2016. Identifying the nature, extent and duration of critical production periods for Atlantic salmon in Macquarie Harbour, Tasmania, during summer. In: *Fisheries Research and Development Corporation Report 229*.
- Endresen, P.C., Klebert, P., 2020. Loads and response on flexible conical and cylindrical fish cages: a numerical and experimental study based on full-scale values. *Ocean Eng.* 216, 107672. <https://doi.org/10.1016/j.oceaneng.2020.107672>.
- Evensen, G., 2003. The ensemble Kalman filter: theoretical formulation and practical implementation. *Ocean Dyn.* 53, 343–367. <https://doi.org/10.1007/s10236-003-0036-9>.
- FAO, 2022. The state of world fisheries and aquaculture 2022. FAO. <https://doi.org/10.4060/cc0461en>.
- Føre, M., Dempster, T., Alfredsen, J.A., Johansen, V., Johansson, D., 2009. Modelling of Atlantic salmon (*Salmo salar* L.) behaviour in sea-cages: a Lagrangian approach. *Aquaculture* 288, 196–204. <https://doi.org/10.1016/j.aquaculture.2008.11.031>.
- Føre, M., Alver, M.O., Alfredsen, J.A., Senneset, G., Espmark, Å., Terjesen, B.F., 2018a. Modelling how the physical scale of experimental tanks affects salmon growth performance. *Aquaculture* 495, 731–737. <https://doi.org/10.1016/j.aquaculture.2018.06.057>.
- Føre, M., Frank, K., Norton, T., Svendsen, E., Alfredsen, J.A., Dempster, T., Berckmans, D., 2018b. Precision fish farming: a new framework to improve production in aquaculture. *Biosyst. Eng.* 173, 176–193. <https://doi.org/10.1016/j.biosystemseng.2017.10.014>.
- Fossen, T.I., 1999. *Guidance and Control of Ocean Vehicles*. University of Trondheim, Norway. Printed by John Wiley & Sons, Chichester, England, ISBN: 0 471 94113 1, Doctors Thesis.

- Grøttum, J.A., Sigholt, T., 1998. A model for oxygen consumption of Atlantic salmon (*Salmo salar*) based on measurements of individual fish in a tunnel respirometer. *Aquac. Eng.* 17, 241–251. [https://doi.org/10.1016/S0144-8609\(98\)00012-0](https://doi.org/10.1016/S0144-8609(98)00012-0).
- Johansson, D., Ruohonen, K., Kiessling, A., Oppedal, F., Stiansen, J.E., Kelly, M., Juell, J. E., 2006. Effect of environmental factors on swimming depth preferences of Atlantic salmon (*Salmo salar* L.) and temporal and spatial variations in oxygen levels in sea cages at a fjord site. *Aquaculture* 254, 594–605. <https://doi.org/10.1016/j.aquaculture.2005.10.029>.
- Johansson, D., Juell, J.E., Oppedal, F., Stiansen, J.E., Ruohonen, K., 2007. The influence of the pycnocline and cage resistance on current flow, oxygen flux and swimming behaviour of Atlantic salmon (*Salmo salar* L.) in production cages. *Aquaculture* 265, 271–287. <https://doi.org/10.1016/j.aquaculture.2006.12.047>.
- Jónsdóttir, K.E., Volent, Z., Alfredsen, J.A., 2021. Current flow and dissolved oxygen in a full-scale stocked fish-cage with and without lice shielding skirts. *Appl. Ocean Res.* 108, 102509 <https://doi.org/10.1016/j.apor.2020.102509>.
- Klebert, P., Lader, P., Gansel, L., Oppedal, F., 2013. Hydrodynamic interactions on net panel and aquaculture fish cages: a review. *Ocean Eng.* 58, 260–274. <https://doi.org/10.1016/j.oceaneng.2012.11.006>.
- Kristiansen, T., Faltinsen, O.M., 2012. Modelling of current loads on aquaculture net cages. *J. Fluids Struct.* 34, 218–235. <https://doi.org/10.1016/j.jfluidstructs.2012.04.001>.
- McIntosh, P., Barrett, L., Warren-Myers, F., Coates, A., Macaulay, G., Szetey, A., Dempster, T., 2022. Supersizing salmon farms in the coastal zone: a global analysis of changes in farm technology and location from 2005 to 2020. *Aquaculture*. <https://doi.org/10.1016/j.aquaculture.2022.738046>.
- Oldham, T., Dempster, T., Fosse, J.O., Oppedal, F., 2017. Oxygen gradients affect behaviour of caged Atlantic salmon *Salmo salar*. *Aquacult. Environ. Interact.* 9, 145–153. <https://doi.org/10.3354/aei00219>.
- Oldham, T., Oppedal, F., Dempster, T., 2018. Cage size affects dissolved oxygen distribution in salmon aquaculture. *Aquacult. Environ. Interact.* 10, 149–156. <https://doi.org/10.3354/aei00263>.
- Oppedal, F., Dempster, T., Stien, L.H., 2011. Environmental drivers of Atlantic salmon behaviour in sea-cages: a review. *Aquaculture* 311, 1–18. <https://doi.org/10.1016/j.aquaculture.2010.11.020>.
- Quiñones, R.A., Fuentes, M., Montes, R.M., Soto, D., León-Muñoz, J., 2019. Environmental issues in Chilean salmon farming: a review. *Rev. Aquac.* 11, 375–402. <https://doi.org/10.1111/raq.12337>.
- Rasheed, A., San, O., Kvamsdal, T., 2020. Digital twin: values, challenges and enablers from a modeling perspective. *IEEE Access* 8, 21980–22012. <https://doi.org/10.1109/access.2020.2970143>.
- Remen, M., Oppedal, F., Imsland, A.K., Olsen, R.E., Torgersen, T., 2013. Hypoxia tolerance thresholds for post-smolt Atlantic salmon: dependency of temperature and hypoxia acclimation. *Aquaculture* 416–417, 41–47. <https://doi.org/10.1016/j.aquaculture.2013.08.024>.
- Remen, M., Sievers, M., Torgersen, T., Oppedal, F., 2016. The oxygen threshold for maximal feed intake of Atlantic salmon post-smolts is highly temperature-dependent. *Aquaculture* 464, 582–592. <https://doi.org/10.1016/j.aquaculture.2016.07.037>.
- Stehfest, K.M., Carter, C.G., McAllister, J.D., Ross, J.D., Semmens, J.M., 2017. Response of Atlantic salmon *Salmo salar* to temperature and dissolved oxygen extremes established using animal-borne environmental sensors. *Sci. Rep.* 7, 1–10. <https://doi.org/10.1038/s41598-017-04806-2>.
- Stockwell, C.L., Filgueira, R., Grant, J., 2021. Determining the effects of environmental events on cultured Atlantic salmon behaviour using 3-dimensional acoustic telemetry. *Front. Anim. Sci.* 2, 26.
- Su, B., Kelasidi, E., Frank, K., Haugen, J., Føre, M., Pedersen, M.O., 2021. An integrated approach for monitoring structural deformation of aquaculture net cages. *Ocean Eng.* 219, 108424 <https://doi.org/10.1016/j.oceaneng.2020.108424>.
- Wang, G.G., 2002. Definition and review of virtual prototyping. *J. Comput. Inf. Sci. Eng.* 2, 232–236. <https://doi.org/10.1115/1.1526508>.